



1 **Formation and growth of atmospheric nanoparticles in the eastern Mediterranean: Results**  
2 **from long-term measurements and process simulations**

3

4 Nikos Kalivitis<sup>1,2</sup>, Veli-Matti Kerminen<sup>3</sup>, Giorgos Kouvarakis<sup>1</sup>, Iasonas Stavroulas<sup>1,4</sup>, Evaggelia  
5 Tzitzikalaki<sup>1</sup>, Panayiotis Kalkavouras<sup>1,5</sup>, Nikolaos Daskalakis<sup>1,6</sup>, Stelios Myriokefalitakis<sup>5,7</sup>,  
6 Aikaterini Bougiatioti<sup>5</sup>, Hanna Elina Manninen<sup>8</sup>, Pontus Roldin<sup>9</sup>, Tuukka Petäjä<sup>3</sup>, Michael Boy<sup>3</sup>,  
7 Markku Kulmala<sup>3</sup>, Maria Kanakidou<sup>1</sup>, and Nikolaos Mihalopoulos<sup>1,5</sup>

8

9 1. Environmental Chemical Processes Laboratory, Chemistry Department, University of Crete,  
10 70013, Heraklion, Greece

11 2. Institute for Astronomy, Astrophysics, Space Applications and Remote Sensing, National  
12 Observatory of Athens, I. Metaxa & Vas. Pavlou, 15236 Palea Penteli, Greece

13 3. Institute for Atmospheric and Earth System Research, Gustaf Hällströmin katu 2, P.O. Box  
14 64, FI-00014 University of Helsinki

15 4. Energy, Environment and Water Research Center, The Cyprus Institute, Nicosia 2121,  
16 Cyprus

17 5. Institute for Environmental Research & Sustainable Development, National Observatory of  
18 Athens, I. Metaxa & Vas. Pavlou, 15236 Palea Penteli, Greece

19 6. Laboratory for Modeling and Observation of the Earth System (LAMOS), Institute of  
20 Environmental Physics (IUP), University of Bremen, Bremen, Germany,

21 7. Institute for Marine and Atmospheric Research (IMAU): Utrecht, Netherlands

22 8. Experimental Physics Department, CERN, 1211 Geneva, Switzerland

23 9. Lund University

24

25

26 *Correspondence to:* Nikos Kalivitis ([nkalivitis@uoc.gr](mailto:nkalivitis@uoc.gr))

27

28



1 Abstract

2 Atmospheric New Particle Formation (NPF) is a common phenomenon all over the world. In  
3 this study we present the longest time series of NPF records in the eastern Mediterranean  
4 region by analyzing seven years of aerosol number size distribution data obtained with a  
5 mobility particle sizer. The measurements were performed at the Finokalia environmental  
6 research station on Crete, Greece during the period June 2008-June 2015. We found that NPF  
7 took place 29% of the available days, undefined days were 26% and non-event days 45%. NPF  
8 is more frequent in April and May probably due to the biogenic activity and is less frequent in  
9 August and November. The NPF frequency increased during the measurement period, while  
10 particle growth rates showed a decreasing trend, indicating possible changes in the ambient  
11 sulfur dioxide concentrations in the area. Throughout the period under study, we frequently  
12 observed production of particles in the nucleation mode during night-time, a feature rarely  
13 observed in the ambient atmosphere. Nucleation mode particles had the highest  
14 concentration in winter, mainly because of the minimum sinks, and their average contribution  
15 to the total particle number concentration was 9%. Nucleation mode particle concentrations  
16 were low outside periods of active NPF and growth, so there are hardly any other local sources  
17 of sub-25 nm particles. Additional atmospheric ion size distribution data simultaneously  
18 collected for more than two years period were also analyzed. Classification of NPF events  
19 based on ion measurements differed from the corresponding classification based on mobility  
20 spectrometer measurements, possibly indicating a different representation of local and  
21 regional NPF events between these two measurement data sets. We used MALTE-box model  
22 for a simulation case study of NPF in the eastern Mediterranean region. Monoterpenes  
23 contributing to NPF can explain a large fraction of the observed NPF events according to our  
24 model simulations. However the parametrization that resulted after sensitivity tests was  
25 significantly different from the one applied for the boreal environment.

26 1) Introduction

27 Most of the atmospheric aerosol particles, and a substantial fraction of particles able to act as  
28 cloud condensation nuclei (CCN), have been estimated to originate from new particle  
29 formation (NPF) taking place in the atmosphere (Spracklen et al. 2006; Kerminen et al., 2012;  
30 Gordon et al., 2017). The exact mechanisms driving atmospheric NPF and subsequent particle  
31 growth processes are still not fully understood, nor are the roles of different vapors and ions  
32 in these processes (Kulmala et al., 2014; Lehtipalo et al., 2016; Tröstl et al., 2016). In order to  
33 understand how aerosol particles affect regional and global climate and air quality, it is



1 necessary to quantify the factors that determine the occurrence of NPF and characterize the  
2 parameters that describe the strength of NPF, such as the new particle formation and growth  
3 rates, in various environments.

4 While NPF has been reported to take place worldwide (Kulmala et al., 2004a; Wang et al.,  
5 2017), observational studies on this subject are scarce in rural sub-tropical environments.  
6 Several studies have investigated NPF in eastern Mediterranean and found it to be a frequent  
7 phenomenon. Lazaridis et al. (2006) first reported NPF at the area and correlated these events  
8 to polluted air masses. Petäjä et al. (2007) presented NPF in Athens metropolitan area and  
9 showed that under the influence of urban pollution, condensing species leading to growth of  
10 the new particles are far more hygroscopic than under cleaner conditions. NPF events have  
11 also been reported to be frequent at the urban environment of Thessaloniki (Siakavaras et al.,  
12 2016). Kalivitis et al. (2008) showed that precursors and nucleation mode particles experience  
13 strong scavenging on Crete island during summer. Pikridas et al. (2012) suggested that  
14 nucleation events occurred only when particles were neutral, being consistent with the  
15 hypothesis that a lack of  $\text{NH}_3$ , during periods when particles are acidic, may limit nucleation in  
16 sulfate-rich environments such as the eastern Mediterranean. Additionally, based on ion  
17 observations, Pikridas et al. (2012) showed that NPF is more frequent in winter. By using the  
18 same data set from eastern Mediterranean, Kalivitis et al. (2012) reported night-time  
19 enhancements in ion concentrations with a plausible association with NPF, being among the  
20 very few locations where such observations have been made. Manninen et al. (2010)  
21 presented an analysis of a full year of observations of NPF with atmospheric ion spectrometers  
22 at various locations across Europe during the EUCAARI project and showed that NPF is less  
23 frequent in the eastern Mediterranean site than in other, mostly continental, European sites.  
24 On the other hand, Berland et al. (2017) showed that similar patterns are being observed  
25 throughout the Mediterranean when comparing observations from the island of Crete to a  
26 western Mediterranean site in terms of the frequency of occurrence, seasonality, and particle  
27 formation and growth rates. Kalivitis et al. (2015) studied for the first time the NPF-CCN link  
28 using observations of particle number size distributions, CCN and high-resolution aerosol  
29 chemical composition for the eastern Mediterranean atmosphere. From the hygroscopicity of  
30 the particles in different size fractions, it was concluded that smaller particles during active  
31 NPF periods tend to be less hygroscopic (and richer in organics) than larger ones. Finally,  
32 Kalkavouras et al. (2017) reported that NPF may result in higher CCN number concentrations,  
33 but the effect on cloud droplet number is limited by the prevailing meteorology.



1 In this work, we present results from the analysis of seven years of aerosol particles number  
2 size distributions and more than two years of atmospheric ion size distributions, representing  
3 the longest published NPF data set in the Mediterranean atmosphere. The main questions we  
4 wanted to address were: 1) How often does NPF take place in eastern Mediterranean, what  
5 are the characteristics of this phenomenon and to what extent has it changed over the period  
6 under study? 2) Are there features in NPF observed at the study area that are not common in  
7 other locations? and 3) How well can numerical models, used in different environmental  
8 conditions, represent NPF in this subtropical environment?

9 2) Materials and methods

10 2.1) Measurements

11 Measurements presented in this work were carried out at the atmospheric observation  
12 station of the University of Crete at Finokalia, Crete, Greece (35°20' N, 25°40' E, 250m a.s.l.)  
13 over seven years, between June 2008 and June 2015. The Finokalia station  
14 (<http://finokalia.chemistry.uoc.gr/>) is a European supersite for aerosol research, part of the  
15 ACTRIS (Aerosols, Clouds, and Trace gases Research Infrastructure) Network. The station is  
16 located at the top of a hill over the coastline, in the north east part of the island of Crete  
17 (Mihalopoulos et al., 1997). The station is representative for the marine background  
18 conditions of eastern Mediterranean (Lelieveld et al., 2002), with negligible influence by local  
19 anthropogenic sources. The nearest major urban center in the area is Heraklion with  
20 approximately 200 000 inhabitants, located about 50 km to the west of the station.

21 In order to monitor the NPF events from the early stages of nucleation, a TROPOS type  
22 custom-built Scanning Mobility Particle Sizer (SMPS), similar to IFT-SMPS in Wiedensohler et  
23 al. (2012), was used at Finokalia. Particle number size distributions were measured in the  
24 diameter range of 9–848 nm every five minutes. The system was a closed-loop, with a 5:1  
25 ratio between the aerosol and sheath flow and it consists of a Kr-85 aerosol neutralizer (TSI  
26 3077), a Hauke medium Differential Mobility Analyzer (DMA) and a TSI-3772 Condensation  
27 Particle Counter (CPC). The sampling was made through a PM<sub>10</sub> sampling head and the sample  
28 humidity was regulated below the relative humidity of 40% with the use of Nafion® dryers in  
29 both the aerosol and sheath flow. The measured number size distributions were corrected for  
30 particle losses by diffusion on the various parts of the SMPS according to the methodology  
31 described in Wiedensohler et al. (2012). Three different types of calibration were performed  
32 for the SMPS, DMA voltage supply calibration, aerosol and sheath flows calibrations and size



1 calibrations. These measurements have been performed at Finokalia on a continuous basis  
2 since 2008. The instrument used at Finokalia was audited on-site with good results in the  
3 framework of EUSAAR (European Supersites for Atmospheric Aerosol Research) project  
4 (<http://www.wmo-gaw-wcc-aerosol-physics.org/audits.html>) and has successfully passed  
5 twice laboratory intercomparison workshops (2013 and 2016, reports available at  
6 <http://www.wmo-gaw-wcc-aerosol-physics.org/instrumental-workshops.html>) in the  
7 framework of ACTRIS project. The instrument has been operated following the  
8 recommendations described in Wiedensohler et al. (2012). Additional information for newly  
9 formed particles were obtained with the use of an Air Ion Spectrometer (AIS- AIREL Ltd.,  
10 Institute of Environmental Physics, University of Tartu, Estonia). AIS is a cluster ion air  
11 spectrometer used to simultaneously measure electrical mobility distribution of positive and  
12 negative air ions (mobilities in the range of  $2.4$  to  $1.3 \cdot 10^{-3} \text{ cm}^2 \text{ V}^{-1} \text{ s}^{-1}$ ). The mobility distributions  
13 were then transformed to size distributions in the size range  $0.8$ - $42$  nm. The number counting  
14 threshold was approximately  $10 \text{ cm}^{-3}$  and the uncertainties of the AIS measurements were  
15  $\sim 10\%$  for negative and positive ion concentrations and  $\sim 0.5$  nm in size. The diameter of the  
16 AIS inlet tube was  $35$  mm and the sample flow rate was  $60 \text{ L m}^{-1}$ . The time step of the  
17 measurements was five minutes.

18 These measurements have been used to identify NPF for the whole period and provide a  
19 historical perspective for the frequency and the characteristics of NPF phenomena in the  
20 eastern Mediterranean. Calculations for formation rates of new particles (J), growth rates (GR)  
21 in various size ranges and condensation sink (CS) were made according to Kulmala et al.  
22 (2012). Formation rates of particles with diameter  $D$  were calculated as:

$$23 \quad J_{Dp} = \frac{\Delta N_{Dp}}{\Delta t} + CoagS_{Dp} \cdot N_{Dp} + \frac{GR}{\Delta D_p} \cdot N_{Dp} + S_{losses} \quad (1)$$

24  $\Delta N_{Dp}$  is the increase in nucleation mode particles' number concentration ( $D_p < 25 \text{ nm}$ ), CoagS  
25 is the coagulation of particles in this size range, GR is the growth rate in the size range  $9$ - $25 \text{ nm}$ .  
26  $S_{losses}$  takes into account additional losses and was neglected in this study. GR was calculated  
27 using the mode-fitting method. The aerosol size distributions were fitted with lognormal  
28 distributions and the nucleation mode geometric mean diameter was plotted as a function of  
29 time. GR was calculated as the slope of the linear fit so that:

$$30 \quad GR = \frac{dD_p}{dt} \quad (2)$$

31 CS is the sulfuric acid sink caused by the preexisting aerosol population with unit  $\text{s}^{-1}$ .



1 All important meteorological parameters were monitored every five minutes using an  
2 automated meteorological station, including the temperature, wind velocity and direction,  
3 relative humidity, solar irradiance and precipitation. Ozone concentrations were measured  
4 with a TEI 49C instrument and nitrogen oxides with a TEI 42CTL, both commercially available,  
5 with a time step of five minutes.

#### 6 2.2) NPF simulations with the MALTE-Box model

7 The simulations of NPF events in the eastern Mediterranean atmosphere were here  
8 performed using the MALTE-box model of the University of Helsinki. This 0-d model able to  
9 simulate aerosol dynamics and chemical processes has successfully reproduced observations  
10 of aerosol formation and growth in the boreal environment (Boy et al., 2006) as well as in  
11 highly polluted areas (Huang et al., 2016). For the present study, relevant chemical reactions  
12 from the Master Chemical Mechanism were incorporated in the MALTE-box chemical  
13 mechanism, as described in Boy et al. (2013). These include the full MCM degradation scheme  
14 of the following volatile organic compounds (described in more detail in Tzitzikalaki et al.,  
15 2017): C<sub>1</sub>-C<sub>4</sub> alkanes, C<sub>2</sub>-C<sub>3</sub> alkenes, acetylene, isoprene, α- and β-pinene, aromatics,  
16 methanol, dimethyl sulfide, formaldehyde, formic and acetic acids, acetaldehyde,  
17 glycoaldehyde, glyoxal, methylglyoxal, acetone, hydroxyacetone, butanone and marine  
18 amines. The Kinetic PreProcessor (KPP) was used to produce the Fortran code for the  
19 calculations of the concentrations of each individual compound (Damian et al., 2002), except  
20 for those species whose concentrations were manually input from large scale model  
21 simulations.

22 The major aerosol dynamical processes for clear sky atmosphere were simulated by the size-  
23 segregated aerosol model UHMA (University Helsinki Multicomponent Aerosol Model,  
24 Korhonen et al., 2004) implemented in the MALTE-Box model. Measured aerosol number size  
25 distributions were used to initialize UHMA daily, which simulates NPF, coagulation, growth  
26 and dry deposition of particles. UHMA simulated new cluster formation resulting from free  
27 form nucleation. Apart from sulfuric acid, about 20 low-volatility organic compounds (ELVOCs)  
28 and 7 selected semi-volatile organic compounds (SVOCs) were treated as condensing vapours,  
29 following the simplified chemical mechanism presented in Huang et al. (2016). All these  
30 compounds were treated as sulfuric acid and organics and the condensation of organic vapors  
31 was determined by the nano-Kohler theory (Kulmala et al., 2004b).



1 As input to the MALTE-Box model were used the observations at Finokalia station and when  
2 such observations were not available, the results from numerical simulations with the global  
3 3-dimensional chemistry transport model (CTM) TM4-ECPL (Daskalakis et al., 2015, 2016;  
4 Myriokefalitakis et al, 2010, 2016) for Finokalia. Observational data include temperature,  
5 relative humidity, total radiation (meteorological input), ozone (O<sub>3</sub>) and nitrogen oxides (NO<sub>x</sub>)  
6 concentrations as well as aerosol number size distributions. The aerosol number size  
7 distribution measured by the SMPS was used to calculate the condensation sink for H<sub>2</sub>SO<sub>4</sub>  
8 vapors. Due to the lack of detailed measurements of VOC at Finokalia, as a first approximation,  
9 biogenic and anthropogenic concentrations of all the above mentioned VOCs resolved every  
10 3 hours were taken from the TM4-ECPL model.

11 The global TM4-ECPL model was run driven for this study by ECMWF (European Centre for  
12 Medium – Range Weather Forecasts) Interim re–analysis project (ERA – Interim) meteorology  
13 (Dee et al., 2011) of the year 2012 at an horizontal resolution of 3° in longitude x 2° in latitude  
14 with 34 vertical layers up to 0.1 hPa. The model used year-specific meteorology and emissions  
15 of trace gases and aerosols. For this study, that of the year 2012 was used, except for soil NO<sub>x</sub>  
16 and oceanic CO and VOCs emissions which were taken from POET inventory database for the  
17 year 2000 (Granier et al., 2005). TM4-ECPL simulations for this work were performed with a  
18 model time-step of 30 min, and the simulated VOC concentrations every 3-hours were used  
19 as input to MALTE box model; while SO<sub>2</sub> surface levels at Finokalia were taken from Monitoring  
20 Atmospheric Composition and Climate (MACC) data assimilation system (Inness et al., 2013).

21 For the calculations of the photo-dissociation rate coefficient by the MALTE-Box model, the  
22 solar actinic flux (AF) is needed. Unfortunately, AF was not measured at Finokalia in 2012,  
23 therefore AF levels were calculated by the Tropospheric Ultraviolet and visible Radiation  
24 Model (TUV, Madronich, 1993) version v.5 for cloud free conditions. The ability of TUV to  
25 calculate the AF at Finokalia was investigated by comparing observations of photo dissociation  
26 rates of O<sub>3</sub> (JO<sup>1</sup>D) and NO<sub>2</sub> (JNO<sub>2</sub>) and model calculations. The measurements of these photo  
27 dissociation rates were performed by filter radiometers (Meteorologie Consult, Germany).  
28 The JO<sup>1</sup>D was measured at wavelengths <325nm, while for JNO<sub>2</sub> wavelengths <420nm were  
29 used.

30 A series of sensitivity tests of AF to different input parameters was also performed to optimize  
31 the calculations. The model uses extra-terrestrial solar spectral irradiance (200-1000 nm by  
32 0.01nm steps) and computes its propagation through the atmosphere taking into account  
33 multiple scattering and the absorption and scattering due to gases and particles. TUV inputs



1 of interest were surface reflectivity (albedo), O<sub>3</sub> column, Aerosol Optical Depth at 500nm  
2 (AOD), Single Scattering Albedo of aerosol (SSA), NO<sub>2</sub> column, air density. Total O<sub>3</sub> column  
3 values were taken from Ozone Monitoring Instrument (OMI) on the Aura spacecraft of NASA  
4 (Levelt et al., 2006). Aerosol columnar optical properties were obtained from the Aerosol  
5 Robotic Network (AERONET). AOD data were measured at the FORTH\_Crete station which is  
6 located 35 km west of Finokalia (Fotiadi et al., 2006). Data level 1.5 was used (cloud-screened).  
7 Total NO<sub>2</sub> column values were taken from GOME2 and OMI satellites. The calculations were  
8 carried out at wavelength from 280 to 650nm with a resolution of 5nm. Simulations using  
9 surface reflectivity of 0.075 and simulation using O<sub>3</sub> column taken from OMI had the best  
10 correlation with measurements. However, the TUV model still significantly overestimated  
11 JO<sup>1</sup>D and JNO<sub>2</sub> data. Thus, a parameterisation took place following a simple empirical  
12 approach, according to Mogensen et al. (2015) and the ratios between the measured and  
13 modelled (from TUV) photolysis rate were calculated.

### 14 3) Results and discussion

#### 15 3.1) Particle size distribution and its connection with NPF

16 We analyzed all available measurements of number size distributions of atmospheric aerosol  
17 particles measured at Finokalia in order to identify and analyze the NPF phenomenon in the  
18 eastern Mediterranean. The data coverage for the period 2008-2015 was 82 %, providing the  
19 longest time series of size distributions not only in this region but also in the southern Europe  
20 and a unique data base for aerosol physical properties.

21 First, we calculated the total particle number concentration (median concentration was 2138  
22 cm<sup>-3</sup>) and corresponding number concentration in the nucleation mode ( $d_p < 25\text{nm}$ , median 78  
23 cm<sup>-3</sup>), Aitken mode ( $25\text{nm} < d_p < 100\text{nm}$ , median 992 cm<sup>-3</sup>) and accumulation mode ( $d_p > 100\text{nm}$ ,  
24 median 878 cm<sup>-3</sup>). We found that Aitken mode accounted for 46% and accumulation mode  
25 41% of the total particle number concentration, while the nucleation mode accounted only  
26 for 3%. The standard deviation of the nucleation particle number concentration was 537 cm<sup>-3</sup>,  
27 indicating that the abundance of these smallest particles is of episodic nature. The highest  
28 monthly average concentrations of nucleation mode particles were observed during winter  
29 and the lowest ones during summer (Figure 1a). Calculating the median diurnal variability of  
30 the nucleation mode, we can see that there is a clear pattern for all seasons of the year (Figure  
31 2a) with a sudden burst in the number concentration around noon that is most pronounced  
32 in winter and least in summer. Such an observation suggests that the nucleation particle



1 number concentration is controlled by NPF episodes. As can be seen in Figure 2b where a  
2 typical “banana shaped” pattern of an NPF event at Finokalia is presented, the sudden burst  
3 at noon is typical for a NPF event. In summer, nucleation mode particles have the highest  
4 concentrations during the night, yet another concentration relative maximum before noon  
5 can be attributed to NPF (Figure 2a). The shift in the average time of the daytime burst of  
6 nucleation mode particles can be attributed to the annual variation of the daylight length.  
7 Similar observations to ours have been reported in Cusack et al. (2013) for the western  
8 Mediterranean where the diurnal variation of nucleation mode particles presents a clear  
9 maximum at noon under both polluted and clean conditions.

10 It is worth noticing that during night-time the median nucleation mode particle number  
11 concentrations were almost the same in all the seasons. This suggests that there is some new  
12 particle production mechanism at night that operates separately from daytime NPF.  
13 Frequently during the night-time, we observed a pronounced appearance of new nucleation  
14 mode particles over several hours as illustrated by Figure 3. While nocturnal NPF has been  
15 reported in the literature (see Salimi et al. (2017) and references therein), this phenomenon  
16 seems to be rare and it remains unclear what are the exact mechanisms leading to it. Given  
17 that we observed no or little growth during nighttime NPF, we may assume that the sources  
18 leading to the formation of new particles are local rather than regional. Observations of very  
19 localized NPF have been reported in Mace Head, Ireland, where intense NPF frequently takes  
20 place under low tide conditions when algae are exposed to the atmosphere (O’Dowd et al.,  
21 2002). Henceforth, we will exclude the nighttime NPF events from our further analysis. We  
22 refer the interested reader to Kalivitis et al. (2012) for a more detailed description of this  
23 phenomenon.

24 Overall, we observed atmospheric NPF to take place during both day and night at Finokalia,  
25 but no sign of any other source of nucleation mode particles in measured air masses. We  
26 therefore hypothesize that atmospheric NPF is the dominant source of nucleation mode  
27 particles in this Mediterranean environment.

### 28 3.2) Characteristics of NPF in the eastern Mediterranean

29 We analyzed the dataset of aerosol size distributions following the approach of Dal Maso et  
30 al. (2005) in order to mark the available days as 1) NPF event days when a clear new nucleation  
31 mode and subsequent growth of newly-formed particles to larger diameters can be observed,  
32 2) non-event days and 3) undefined days when either new particles appear into the Aitken



1 mode or nucleation mode particles do not show a clear growth. The available days were  
2 manually inspected and classified.

3 We used the Statistica software package for Windows to carry out factor analyses, including  
4 meteorological parameters, ozone concentrations (as the major oxidant in the atmosphere)  
5 and PM<sub>10</sub> mass concentration (as an index of particulate pollutant levels), in order to examine  
6 whether any of these factors were associated with the formation of new particles,  
7 represented by the nucleation mode number concentration. Furthermore, we divided our  
8 data to night and day time periods in order to separate daytime NPF from that taking place  
9 during nighttime. The only parameter that had some effect on the nucleation mode particle  
10 number concentration was the wind velocity: when strong winds were prevailing at Finokalia,  
11 it was more unlikely to observe nucleation particles. On the other hand, the lack of correlation  
12 to any other parameter may indicate that the NPF is not sensitive to local meteorological  
13 conditions or atmospheric chemical composition in this environment. Air mass back  
14 trajectories calculated using the HYSPLIT model showed no major difference during NPF  
15 events from air masses typical for the prevailing situation at Finokalia: air masses arriving at  
16 Finokalia from the northeast were the most frequent during NPF events (27% against 24% of  
17 all days), followed by northwestern air masses that were more frequent than the average  
18 (21% against 17%) and northern directions (18% against 20%).

19 Next, we focused on determining the main characteristics of daytime NPF at Finokalia. Overall,  
20 623 NPF events were identified. This is the longest time series of the NPF phenomenon  
21 recorded in the Mediterranean atmosphere, providing a representative climatology of NPF  
22 events in this region. NPF took place 29% of the 2121 available measurement days whereas  
23 no event occurred on 45% of those days. It is worth noting that 26% of the days were  
24 characterized as undefined, which means that while no clear NPF event could be observed,  
25 there was some evidence of secondary particle formation although not at the immediate  
26 vicinity of the station (Table 1). We found that NPF is most frequent in April and May, probably  
27 due to the biogenic activity, and least frequent in August and November (Figure 4) probably  
28 due to high wind speeds occurring these months from NE and S/SW directions respectively  
29 (not shown). Nevertheless, NPF takes place throughout the year. One would expect NPF to be  
30 most frequent in winter when the highest concentrations of nucleation particles are observed,  
31 however this was not the case. A possible explanation for the high nucleation mode particle  
32 number concentrations in winter could be that the probability of a newly formed particle to  
33 survive is larger than in other times of the year. The survival probability of newly-formed



1 particles is closely related to the ratio GR/CS (Kerminen and Kulmala, 2002; Kulmala et al.,  
2 2017). By looking at the seasonal variability of CS and GR (Figures 1b and 6b), the particle  
3 survival probability seems to be the highest in winter.

4 As a next step, we classified the NPF events into Class I or Class II events depending on whether  
5 the particle formation rate at 9 nm ( $J_9$ ) and growth rates from 9 to 25 nm diameter ( $GR_{9-25}$ )  
6 could be calculated with a good confidence. Overall, Class I events corresponded to 8% of the  
7 available measuring days and 26% of the event days, and they were observed throughout the  
8 year, providing enough data for a statistical analysis of particle formation and growth rates  
9 during NPF events (Figure 5).

10 The average value of  $J_9$  during the Class I NPF events in Finokalia was  $1.1 \pm 1.6 \text{ cm}^{-3} \text{ s}^{-1}$  (median  
11  $0.5 \text{ cm}^{-3} \text{ s}^{-1}$ ). This is well in the range of values reported for  $J_{10}$  in other locations (Kulmala et  
12 al., 2004a), higher though than  $J_{16}$  reported by Berland et al. (2017) at the Finokalia site in  
13 2013 ( $0.26 \text{ cm}^{-3} \text{ s}^{-1}$ ), but substantially lower than the values found by Kopanakis et al. (2013)  
14 in western Crete ( $13.1 \pm 9.9 \text{ cm}^{-3} \text{ s}^{-1}$ ). The monthly variation of  $J_9$  (Figure 6a) shows that the  
15 highest formation rates were observed in November and March. The spring maximum in the  
16 particle formation rate might be due to the enhanced biogenic activity and increasing  
17 photochemical activity. The November maximum might appear as a result of the initiation of  
18 the rain season at Crete and the subsequent rapid drop in CS, even though it is very difficult  
19 to say which factors determine the monthly variability of  $J_9$  at Finokalia. Seasonal averages of  
20  $J_9$ ,  $GR_{9-25}$  and CS are summarized in Table 2. Moreover, we found that  $J_9$  and  $N_{9-25}$  have a clear  
21 linear relation (Figure 7), which supports our earlier hypothesis that at Finokalia the main  
22 source of nucleation mode particles is their secondary formation in the atmosphere.

23 We calculated the average growth rate of the newly formed particles to be  $5.1 \pm 3.9 \text{ nm hr}^{-1}$   
24 (median  $4.1 \text{ nm hr}^{-1}$ ). We found that  $GR_{9-25}$  is highest in summer and lowest in winter and early  
25 spring, probably in line with the seasonal cycle of photochemical activity and biogenic  
26 emission patterns, producing condensable species that are driving the growth process (Figure  
27 6b). The average duration of the NPF in summer seems to be shorter as shown in Figure 2a  
28 and that may be explained by the higher growth rates observed.

### 29 3.3) NPF trends during the 2008-2015 period

30 By looking at the inter-annual evolution of the NPF monthly event frequency at Finokalia for  
31 the 85 available months, we observe a slight increase of about 1.5 % per year (Figure 8a). This  
32 trend is not statistically significant since p-value was found to be 0.07. This increase is a result



1 of a notable increase of Class II NPF events despite a simultaneous decrease of Class I events  
2 from 2008 to 2015 (8b). During the measurement period under study, no trend in  $J_9$  was  
3 observed, but the winters 2008-9 and 2012-13 had clearly higher values of  $J_9$  than the rest of  
4 the time (Figure 8c).

5 When looking at the temporal variation of GR (Figure 8d), we observe a clear decreasing trend  
6 of about  $0.3 \text{ nm hr}^{-1} \text{ yr}^{-1}$ . This trend can be considered statistically significant, the no-trend  
7 hypothesis test returned a p-value of 0.03. In order to explain this trend, we need to  
8 emphasize the regional characteristics of the observations at Finokalia, as this site is greatly  
9 affected by long-range transported pollutants of marine, desert dust and polluted continental  
10 origin (Lelieveld et al., 2002). Non-sea salt sulfate ( $\text{nss-SO}_4^{2-}$ ) can be considered as an indicator  
11 of regional pollution from anthropogenic activities ( $\text{SO}_2$  emissions), and since the beginning of  
12 the economic crisis in Europe, especially in Greece, we can observe a clear decline in its  
13 concentration (Paraskevopoulou et al., 2015). We can therefore assume also a regional  
14 decrease in  $\text{SO}_2$  emissions, since a major part of  $\text{SO}_2$  at Finokalia can be attributed to  
15 transported pollution (Sciare et al., 2003). This would result in a decrease in the availability of  
16 sulfuric acid, a major condensable species responsible for the particle growth (Bzdek et al.,  
17 2012).

18 Hamed et al. (2010) studied the effect of the reduction in anthropogenic  $\text{SO}_2$  emissions in  
19 Germany between the years 1996-97 and 2003-06 as a result of the socio-economic changes  
20 in East Germany after the reunification. They observed a notable decrease in the NPF event  
21 frequency but an increase in the growth rate of nucleated particles. A decrease in the NPF  
22 frequency due to the reduction of anthropogenic  $\text{SO}_2$  emissions in eastern Lapland was  
23 observed by Kyrö et al. (2014), and this decrease was most pronounced for the Class I NPF  
24 events. Nieminen et al. (2014) analyzed the longest data set reported in literature from  
25 Finland and found that, despite major decreases in ambient  $\text{SO}_2$  concentrations observed all  
26 over Europe as a result of overall air quality improvements, there was a slight upward trend  
27 in the particle formation and growth rates. This feature was attributed partly to increased  
28 biogenic emissions over the same period. Taken together, we conclude that the observed  
29 decrease in the particle growth rate and frequency in the most pronounced NPF events in  
30 Finokalia could as well be due to decreased  $\text{SO}_2$  concentrations. The reasons for the overall  
31 increase in the NPF frequency and little change in  $J_9$  remain unclear, even though factors like  
32 meteorological conditions and organic vapor abundance have probably played some role in  
33 this respect.



1 3.4) Atmospheric ion observations related to new particle formation

2 At the Finokalia station, atmospheric ion observations relevant to new particle formation were  
3 performed during two separate periods, 2008-2009 during the EUCAARI project (Manninen et  
4 al., 2010) and 2012-2014 during the FRONT (Formation and growth of atmospheric  
5 nanoparticles) project. Here we will focus only on FRONT data, since the EUCAARI dataset is  
6 discussed in detail in Manninen et al. (2010) and Pikridas et al., (2012). A typical nucleation  
7 event is presented in Fig. 9 as recorded by both the AIS and SMPS. AIS observations may  
8 provide information about the initial stages of new particle formation as particles can be  
9 observed emerging in the intermediate ion diameter range 1.6-7.4 nm. Intermediate ions  
10 appear only under certain circumstances, such as during precipitation, at high wind speeds,  
11 and when NPF is taking place (Hörrak et al. 1998; Tammet et al., 2014; Leino et al., 2016; Chen  
12 et al., 2017). In the following we will focus on NPF and use only the observations from the  
13 negative polarity due to the better representation of NPF events in those data compared with  
14 corresponding positive ions in our dataset (Figure 9).

15 We classified all of the available AIS measurement days into event, non-event and undefined  
16 days, once again according to methods introduced by Dal Maso et al. (2005), and subsequently  
17 compared the findings from AIS data to those from the SMPS data. Surprisingly, the two data  
18 sets for the same time period gave quite different results in terms of the NPF event frequency:  
19 in the AIS data the NPF event frequency peaked earlier during the year than in the SMPS data  
20 (Figure 10). This feature was evident in both periods of AIS measurements and is probably due  
21 to the different measurement characteristics of the AIS and SMPS instruments. For example,  
22 it is possible that AIS data are more representative of local NPF events with limited particle  
23 growth, and such events may not be seen in the SMPS data. On the other hand, the SMPS  
24 measures neutral particles but has a much higher detection limit (9nm), so its data may be  
25 more representative of regional NPF that takes place over distances of hundreds of kilometers  
26 (Kalkavouras et al., 2017).

27 We calculated the growth rates at three different size ranges for the FRONT project similarly  
28 to Manninen et al. (2010) and Pikridas et al (2012) for the EUCAARI project data. The particle  
29 growth rates in the size ranges 1.5-3 nm, 3-7nm and 7-20 nm were  $1.6 \pm 1.8 \text{ nm hr}^{-1}$ ,  $5.4 \pm 4.9$   
30  $\text{nm hr}^{-1}$  and  $9.1 \pm 9.5 \text{ nm hr}^{-1}$ , respectively. These values are lower than those in Pikridas et al.  
31 (2012) but comparable to those observed during the EUCAARI project for the first two size  
32 ranges, and higher than those observed during the EUCAARI project for the last size range  
33 (Manninen et al., 2010). Overall, we observed much faster growth of newly-formed charged



1 particles in the eastern Mediterranean atmosphere after their first growth steps beyond 3 nm  
2 in diameter, reflecting probably the strong Kelvin effect at small particle sizes preventing  
3 condensation and hence growth, and the abundance of precursors leading to nucleation and  
4 condensing species contributing to each growth stage.

### 5 3.5) Simulations of NPF using the zero-dimensional model MALTE-box

6 In order to evaluate our understanding of the observed NPF events in the eastern  
7 Mediterranean we chose to simulate two distinct cases of one week duration each, during  
8 which NPF events have been observed (event week) or not (no event week). The selection was  
9 done from the summer of the year 2012, when  $\text{JO}^{1\text{D}}$  and  $\text{JNO}_2$  photodissociation  
10 measurements were also available at Finokalia. Two weeks in August 2012 were chosen,  
11 28/08– 03/09 as event week and 09/08– 15/08 as non-event week. The “event week” was  
12 described in detail by Kalivitis et al. (2015). Applying the MALTE-Box model the aerosol size  
13 distribution and its evolution over the week has been simulated for these two cases.

14 During the “event week” the simulated formation of new particles successfully coincided with  
15 the observations, as shown in Figures 11a and 11b. The NPF levels simulated using the  
16 nucleation rates as parameterized for the boreal environment overestimated the  
17 observations while the simulated growth of newly-formed particles was greatly  
18 underestimated as shown in Tzitzikalaki et al. (2017). The most likely reason for this is the very  
19 low concentration of monoterpenes, calculated by TM4-ECPL global model for the Finokalia  
20 model grid box, on which the ELVOC and SVOC chemistry was built on. Indeed, the TM4-ECPL  
21 model results for Finokalia were too low compared to monoterpenes observations in 2014  
22 (not shown). Therefore, we performed a number of sensitivity tests to improve the  
23 simulations. The best agreement between model results and observations was reached by  
24 decreasing the nucleation coefficient from  $10^{-11} \text{ s}^{-1}$  (the value commonly used for the boreal  
25 environment) to  $5 \times 10^{-16} \text{ s}^{-1}$  and increasing by a factor of 10 the  $\alpha$ - and  $\beta$ -pinene  
26 concentrations. With these modifications the model results greatly improved and the aerosol  
27 number size distributions were well captured, as well as total number and volume  
28 concentration of aerosol particles (Figures 11c and d respectively). This was the first time that  
29 we were able to simulate in such detail NPF in the eastern Mediterranean. The almost five  
30 orders of magnitude lower nucleation coefficient used here for the sub-tropical set-up could  
31 be related to the contribution of still unknown compounds in the cluster-formation process.  
32 Huang et al. (2016) applied different kinetic nucleation coefficients at Nanjing, China, with the  
33 lowest value for a “China-clean” day of  $6.0 \times 10^{-13} \text{ s}^{-1}$ .



1 Using the non-event week as our control case, we performed simulations of number size  
2 distributions at Finokalia station using the sub-tropical set-up and compared it to our  
3 measurements. For the “non-event week”, weak NPF were predicted by the model during the  
4 last two days that were not found in the measurements (Tzitzikalaki et al., 2017) but appear  
5 to be associated with the rapid drop of CS during day five of the simulations. Nevertheless,  
6 even if no NPF took place during the last two days, it was apparent in our measurements that  
7 some nucleation particles appeared ( $\sim 200 \text{ cm}^{-3}$ ) and thus the general tendency was captured  
8 by the model. Both total number and volume concentrations were well captured by the model  
9 (Figures 12 a, b). These results show the potential of MALTE-box model to simulate the NPF  
10 in the eastern Mediterranean and the importance of input data. Therefore, when more  
11 appropriate input data for Malte-box will become available (concurrent detailed  
12 measurements of gases and aerosol distributions) at Finokalia, new detailed simulations will  
13 further provide insight in NPF phenomena and the factors controlling them in the eastern  
14 Mediterranean atmosphere.

15

#### 16 4) Conclusions

17 NPF in the atmosphere is a recurrent phenomenon in eastern Mediterranean. In this study,  
18 we presented the longest time series of NPF records in the region. We analyzed 2121 days of  
19 aerosol number size distribution data from June 2008 until June 2015 and found that NPF took  
20 place 29% of the available days, more frequently in spring and less frequently in late summer  
21 and autumn. Production of nucleation mode particles was common during night-time as well.  
22 Nucleation mode particle number concentrations were low outside periods of active NPF and  
23 subsequent particle growth indicating absence of local sources. Classification of NPF events  
24 based on atmospheric ion measurements differed from the corresponding classification based  
25 on mobility spectrometer measurements: the maximum frequency of NPF events was  
26 observed earlier in spring from AIS data than from SMPS data, possibly indicating a different  
27 representation of local and regional NPF events between these two data sets since SMPS  
28 measures new particles after they have grown to diameters larger than 9nm and hence  
29 records only regional events lasting for several hours.

30 During the measurement period, the frequency of NPF occurrence increased by 1.5 % per year  
31 while the average GR decreased by  $0.3 \text{ nm hr}^{-1} \text{ yr}^{-1}$ , probably reflecting the decrease of  
32 ambient  $\text{SO}_2$  concentrations due to the economic crisis. We used the MALTE-box model to



1 simulate NPF observations in the eastern Mediterranean region. Using a “sub-tropical”  
2 environment parametrization, we were able to simulate with good agreement the selected  
3 time period. The parametrization used was significantly different than the one used for the  
4 boreal environment: nucleation rates were much lower, yet monoterpenes seemed to play a  
5 key role in the mechanisms governing NPF phenomena.

6 From the results presented in this work it is evident that the Finokalia site is a unique location  
7 in the eastern Mediterranean for studying the processes leading to NPF in the marine  
8 environment. As a next step, a more detailed look to the precursors driving these processes is  
9 necessary, with special emphasis on VOCs, and the expansion of the available measurements  
10 at the site in order to eliminate the uncertainties introduced in our simulations from the use  
11 of model outputs instead of observations.

#### 12 5) Acknowledgements

13 The research project was implemented within the framework of the Action «Supporting  
14 Postdoctoral Researchers» of the Operational Program "Education and Lifelong Learning"  
15 (Action's Beneficiary: General Secretariat for Research and Technology), and was co-financed  
16 by the European Social Fund (ESF) and the Greek State. This research is supported by the  
17 Academy of Finland Center of Excellence program (project number 1118615). We  
18 acknowledge funding from the EU FP7-ENV-2013 program “impact of Biogenic vs.  
19 Anthropogenic emissions on Clouds and Climate: towards a Holistic UnderStanding”  
20 (BACCHUS), project no. 603445 and the Horizon 2020 research and innovation programme  
21 ACTRIS-2 Integrating Activities (grant agreement No. 654109). This study contributes to  
22 ChArMEx work package 1 on aerosol sources.

23



- 1 6) References
- 2 Berland, K., Rose, C., Pey, J., Culot, A., Freney, E., Kalivitis, N., Kouvarakis, G., Cerro, J. C.,
- 3 Mallet, M., Sartelet, K., Beckmann, M., Bourriane, T., Roberts, G., Marchand, N.,
- 4 Mihalopoulos, N., and Sellegri, K.: Spatial extent of new particle formation events over the
- 5 Mediterranean Basin from multiple ground-based and airborne measurements, *Atmos. Chem.*
- 6 *Phys.*, 17, 9567–9583, <https://doi.org/10.5194/acp-17-9567-2017>, 2017.
- 7 Boy, M., Hellmuth, O., Korhonen, H., Nilsson, D., ReVelle, D., Turnipseed, A., Arnold, F. and
- 8 Kulmala, M.: MALTE – Model to predict new aerosol formation in the lower troposphere,
- 9 *Atmos. Chem. Phys.*, 6, 4499–4517, doi:10.5194/acp-6-4499-2006, 2006.
- 10 Boy, M., Mogensen, D., Smolander, S., Zhou, L., Nieminen, T., Paasonen, P., Plass-Dülmer, C.,
- 11 Sipilä, M., Petäjä, T., Mauldin, L., Berresheim, H., and Kulmala, M.: Oxidation of SO<sub>2</sub> by
- 12 stabilized Criegee intermediate (sCI) radicals as a crucial source for atmospheric sulfuric acid
- 13 concentrations, *Atmos. Chem. Phys.*, 13, 3865–3879, [https://doi.org/10.5194/acp-13-3865-](https://doi.org/10.5194/acp-13-3865-2013)
- 14 2013, 2013.
- 15 Bzdek, B. R., Zordan, C. A., Pennington, M. R., Luther, G. W., and Johnston, M. V.: Quantitative
- 16 Assessment of the Sulfuric Acid Contribution to New Particle Growth. *Environmental Science*
- 17 *& Technology*, 46, 4365–4373. <http://doi.org/10.1021/es204556c>, 2012.
- 18 Chen, X., Virkkula, A., Kerminen, V.-M., Manninen, H. E., Busetto, M., Lanconelli, C., Lupi, A.,
- 19 Vitale, V., Del Guasta, M., Grigioni, P., Väänänen, R., Duplissy, E.-M., Petäjä, T., and Kulmala,
- 20 M.: Features of air ions measured by an air ion spectrometer (AIS) at Dome C, *Atmos. Chem.*
- 21 *Phys.*, 17, 13783–13800, 2017.
- 22 Cusack, M., Pérez, N., Pey, J., Wiedensohler, A., Alastuey, A., and Querol, X.: Variability of sub-
- 23 micrometer particle number size distributions and concentrations in the Western
- 24 Mediterranean regional background. *Tellus B*, 65,
- 25 doi:<http://dx.doi.org/10.3402/tellusb.v65i0.19243>, 2013.
- 26 Dal Maso, M., Kulmala, M., Riipinen, I., Wagner, R., Hussein, T., Aalto, P. P., and Lehtinen, K.
- 27 E. J.: Formation and growth of fresh atmospheric aerosols: eight years of aerosol size
- 28 distribution data from SMEAR II, Hyytiälä, Finland, *Boreal Environ. Res.*, 10, 323–336, 2005.



- 1 Damian, V., Sandu, A., Damian, M., Potra, F., and Carmichael, G. R.: The kinetic preprocessor  
2 KPP-a software environment for solving chemical kinetics, *Computers & Chemical*  
3 *Engineering*, 26, 1567–1579, [http://doi.org/10.1016/S0098-1354\(02\)00128-X](http://doi.org/10.1016/S0098-1354(02)00128-X), 2002.
- 4 Daskalakis, N., Myriokefalitakis, S., and Kanakidou, M.: Sensitivity of tropospheric loads and  
5 lifetimes of short lived pollutants to fire emissions, *Atmos. Chem. Phys.*, 15, 3543-3563,  
6 <https://doi.org/10.5194/acp-15-3543-2015>, 2015.
- 7 Daskalakis, N., Tsigaridis, K., Myriokefalitakis, S., Fanourgakis, G. S., and Kanakidou, M.: Large  
8 gain in air quality compared to an alternative anthropogenic emissions scenario, *Atmos.*  
9 *Chem. Phys.*, 16, 9771-9784, doi:10.5194/acp-16-9771-2016, 2016.
- 10 Dee, D. P., Uppala, S. M., Simmons, A. J., Berrisford, P., Poli, P., Kobayashi, S., and Vitart, F.:  
11 The ERA-Interim reanalysis: configuration and performance of the data assimilation system,  
12 *Quarterly Journal of the Royal Meteorological Society*, 137, 553–597.  
13 <http://doi.org/10.1002/qj.828>, 2011.
- 14 Fotiadi, A., Hatzianastassiou, N., Drakakis, E., Matsoukas, C., Pavlakis, K. G., Hatzidimitriou, D.,  
15 Gerasopoulos, E., Mihalopoulos, N., and Vardavas, I.: Aerosol physical and optical properties  
16 in the eastern Mediterranean Basin, Crete, from Aerosol Robotic Network data, *Atmos. Chem.*  
17 *Phys.*, 6, 5399-5413, <https://doi.org/10.5194/acp-6-5399-2006>, 2006.
- 18 Gordon, H., Kirkby, J., Baltensperger, U., Bianchi, F., Breitenlecher, M., Curtius, J., Dias, A.,  
19 Dommen, J., Donahue, N. M., Dunne, E. M., Duplissy, J., Ehrhart, S., Flagan, R. C., Frege, C.,  
20 Fuchs, C., Hansel, A., Hoyle, C. R., Kulmala, M., Kürten, A., Lehtipalo, K., Makhmutov, V.,  
21 Molteni, U., Rissanen, M. P., Stozkhov, Y., Tröstl, J., Tsagkogeorgas, G., Wagner, R., Williamson,  
22 C., Wimmer, D., Winkler, P. M., Yan, C., and Carslaw, K. S.: Causes and importance of new  
23 particle formation in the present-day and preindustrial atmospheres, *J. Geophys. Res. Atmos.*,  
24 122, 8739-8760, 2017.
- 25 Granier, C., Guenther, A., Lamarque, J., Mieville, A., Müller, J., Olivier, J., Orlando, J., Peters,  
26 J., Petron, G., Tyndall, G., and Wallens, S.: POET, a database of surface emissions of ozone  
27 precursors, available at: <http://www.aero.jussieu.fr/projet/ACCENT/POET.php>, 2005.
- 28 Hamed, A., Birmili, W., Joutsensaari, J., Mikkonen, S., Asmi, A., Wehner, B., Spindler, G.,  
29 Jaatinen, A., Wiedensohler, A., Korhonen, H., Lehtinen, K. E. J., and Laaksonen, A.: Changes in  
30 the production rate of secondary aerosol particles in Central Europe in view of decreasing SO<sub>2</sub>



- 1 emissions between 1996 and 2006, Atmos. Chem. Phys., 10, 1071-1091,  
2 <https://doi.org/10.5194/acp-10-1071-2010>, 2010.
- 3 Hörrak U., Salm J., and Tammet H.: Bursts of intermediate ions in atmospheric air, J. Geophys.  
4 Res., 103, 13909–13915, doi: 10.1029/97JD01570, 1998.
- 5 Huang, X., Zhou, L., Ding, A., Qi, X., Nie, W., Wang, M., Chi, X., Petäjä, T., Kerminen, V.-M.,  
6 Roldin, P., Rusanen, A., Kulmala, M., and Boy, M.: Comprehensive modelling study on  
7 observed new particle formation at the SORPES station in Nanjing, China, Atmos. Chem. Phys.,  
8 16, 2477-2492, <https://doi.org/10.5194/acp-16-2477-2016>, 2016.
- 9 Inness, A., Baier, F., Benedetti, A., Bouarar, I., Chabrillat, S., Clark, H., Clerbaux, C., Coheur, P.,  
10 Engelen, R. J., Errera, Q., Flemming, J., George, M., Granier, C., Hadji-Lazaro, J., Huijnen, V.,  
11 Hurtmans, D., Jones, L., Kaiser, J. W., Kapsomenakis, J., Lefever, K., Leitão, J., Razinger, M.,  
12 Richter, A., Schultz, M. G., Simmons, A. J., Suttie, M., Stein, O., Thépaut, J.-N., Thouret, V.,  
13 Vrekoussis, M., Zerefos, C., and the MACC team: The MACC reanalysis: an 8 yr data set of  
14 atmospheric composition, Atmos. Chem. Phys., 13, 4073-4109, [https://doi.org/10.5194/acp-](https://doi.org/10.5194/acp-13-4073-2013)  
15 [13-4073-2013](https://doi.org/10.5194/acp-13-4073-2013), 2013.
- 16 Kalivitis, N., Birmili, W., Stock, M., Wehner, B., Massling, A., Wiedensohler, A., Gerasopoulos,  
17 E., and Mihalopoulos, N.: Particle size distributions in the eastern Mediterranean troposphere,  
18 Atmos. Chem. Phys., 8, 6729-6738, doi:10.5194/acp-8-6729-2008, 2008.
- 19 Kalivitis N., Stavroulas I., Bougiatioti A., Kouvarakis G., Gagné S., Manninen H.E., Kulmala M.,  
20 and Mihalopoulos N.: Night-time enhanced atmospheric ion concentrations in the marine  
21 boundary layer, Atmos. Chem. Phys., 12, 3627-3638, doi:10.5194/acp-12-3627-2012, 2012.
- 22 Kalivitis, N., Kerminen, V.-M., Kouvarakis, G., Stavroulas, I., Bougiatioti, A., Nenes, A.,  
23 Manninen, H. E., Petäjä, T., Kulmala, M., and Mihalopoulos, N.: Atmospheric new particle  
24 formation as a source of CCN in the eastern Mediterranean marine boundary layer, Atmos.  
25 Chem. Phys., 15, 9203-9215, doi:10.5194/acp-15-9203-2015, 2015.
- 26 Kalkavouras, P., Bossioli, E., Bezantakos, S., Bougiatioti, A., Kalivitis, N., Stavroulas, I.,  
27 Kouvarakis, G., Protonotariou, A. P., Dandou, A., Biskos, G., Mihalopoulos, N., Nenes, A., and  
28 Tombrou, M.: New particle formation in the southern Aegean Sea during the Etesians:  
29 importance for CCN production and cloud droplet number, Atmos. Chem. Phys., 17, 175-192,  
30 <https://doi.org/10.5194/acp-17-175-2017>, 2017.



- 1 Kerminen, V.-M. and Kulmala, M.: Analytical formulae connecting the “real” and the  
2 “apparent” nucleation rate and the nuclei number concentration for atmospheric nucleation  
3 events, *J. Aerosol Sci.*, 33, 609-622, 2002.
- 4 Kerminen, V.-M., Paramonov, M., Anttila, T., Riipinen, I., Fountoukis, C., Korhonen, H., Asmi,  
5 E., Laakso, L., Lihavainen, H., Swietlicki, E., Svenningsson, B., Asmi, A., Pandis, S. N., Kulmala,  
6 M., and Petäjä, T.: Cloud condensation nuclei production associated with atmospheric  
7 nucleation: a synthesis based on existing literature and new results, *Atmos. Chem. Phys.*, 12,  
8 12037–12059, doi:10.5194/acp-12-12037-2012, 2012.
- 9 Kopanakis, I., Chatoutsidou, S. E., Tørseth, K., Glytsos, T., and Lazaridis, M.: Particle number  
10 size distribution in the eastern Mediterranean: Formation and growth rates of ultrafine  
11 airborne atmospheric particles, *Atmospheric Environment*, 77, 790–802.  
12 <http://doi.org/10.1016/j.atmosenv.2013.05.066>, 2013.
- 13 Korhonen, H., Lehtinen, K. E. J., and Kulmala, M.: Multicomponent aerosol dynamics model  
14 UHMA: model development and validation, *Atmos. Chem. Phys.*, 4, 757-771,  
15 <https://doi.org/10.5194/acp-4-757-2004>, 2004.
- 16 Kulmala, M., Vehkamäki, H., Peňaja, T., Dal Maso, M., Lauri, A., Kerminen, V.-M., Birmili, W.,  
17 and McMurry, P. H.: Formation and growth rates of ultrafine atmospheric particles: A review  
18 of observations, *J. Aerosol Sci.*, 35, 143–176, 2004a.
- 19 Kulmala, M., Kerminen, V.-M., Anttila, T., Laaksonen, A. and O’Dowd, C. D: Organic aerosol  
20 formation via sulphate cluster activation, *J. Geophys. Res.*, 109, 4205,  
21 doi:10.1029/2003JD003961, 2004b.
- 22 Kulmala, M., Petäjä, T., Nieminen, T., Sipilä, M., Manninen, H. E., Lehtipalo, K., Kerminen, V.-  
23 M.: Measurement of the nucleation of atmospheric aerosol particles, *Nature Protocols*, 7,  
24 1651, <http://dx.doi.org/10.1038/nprot.2012.091>, 2012.
- 25 Kulmala, M., Petäjä, T., Ehn, M., Thornton, J., Sipilä, M., Worsnop, D. R., and Kerminen, V.-M.:  
26 Chemistry of atmospheric nucleation: On the recent advances on precursor characterization  
27 and atmospheric cluster composition in connection with atmospheric new particle formation,  
28 *Annu. Rev. Phys. Chem.*, 65, 21-37, 2014.



- 1 Kulmala, M., Kerminen, V.-M., Petäjä, T., Ding, A. J., and Wang L.: Atmospheric gas-to-particle  
2 conversion: why NPF events are observed in megacities?, *Faraday Discuss.*, 200, 271-288,  
3 doi:10.1039/c6fd00257a, 2017.
- 4 Kyrö, E.-M., Väänänen, R., Kerminen, V.-M., Virkkula, A., Petäjä, T., Asmi, A., Dal Maso, M.,  
5 Nieminen, T., Juhola, S., Shcherbinin, A., Riipinen, I., Lehtipalo, K., Keronen, P., Aalto, P. P.,  
6 Hari, P., and Kulmala, M.: Trends in new particle formation in eastern Lapland, Finland: effect  
7 of decreasing sulfur emissions from Kola Peninsula, *Atmos. Chem. Phys.*, 14, 4383-4396,  
8 <https://doi.org/10.5194/acp-14-4383-2014>, 2014.
- 9 Lazaridis, M., K. Eleftheriadis, J. Smolik, I. Colbeck, G. Kallos, Y. Drossinos, V. Zdimal, Z. Vecera,  
10 N. Mihalopoulos, P. Mikuska, C. Bryant, C. Housiadas, A. Spyridaki, M. Astitha and V. Havranek:  
11 Dynamics of fine particles and photo-oxidants in the eastern Mediterranean (SUB-AERO),  
12 *Atmospheric Environment*, 40, P 6214-6228,  
13 <http://dx.doi.org/10.1016/j.atmosenv.2005.06.050>, 2006.
- 14 Lehtipalo, K., Rondo, L., Kontkanen, J., Schobesberger, S., Jokinen, T., Sarnela, N., Kürten, A.,  
15 Ehrhart, S., Franchin, A., Nieminen, T., Riccobono, F., Sipilä, M., Yli-Juuti, T., Duplissy, J.,  
16 Adamov, A., Ahlm, L., Almeida, J., Amorim, A., Bianchi, F., Breitenlechner, M., Dommen, J.,  
17 Downard, A. J., Dunne, E. M., Flagan, R. C., Guida, R., Hakala, J., Hansel, A., Jud, W.,  
18 Kangasluoma, J., Kerminen, V.-M., Keskinen, H., Kim, J., Kirkby, J., Kupc, A., Kupiainen-Määttä,  
19 O., Laaksonen, A., Lawler, M. J., Leiminger, M., Mathot, S., Olenius, T., Ortega, I. K., Onnela,  
20 A., Petäjä, T., Praplan, A., Rissanen, M. P., Ruuskanen, T., Santos, F. D., Schallhart, S.,  
21 Schnitzhofer, R., Simon, M., Smith, J. N., Tröstl, J., Tsagkogeorgas, G., Tomé, A., Vaattovaara,  
22 P., Vehkamäki, H., Vrtala, A. E., Wagner, P. E., Williamson, C., Wimmer, D., Winkler, P. M.,  
23 Virtanen, A., Donahue, N. M., Carslaw, K. S., Baltensperger, U., Riipinen, I., Curtius, J.,  
24 Worsnop, D. R., and Kulmala, M.: The effect of acid-base clustering and ions on the growth of  
25 atmospheric nano-particles, *Nat. Commun.*, 7, 11594, doi:10.1038/ncomms11594, 2016.
- 26 Leino, K., Nieminen, T., Manninen, H.E., Petäjä, T., Kerminen, V.-M., and Kulmala, M.:  
27 Intermediate ions as a strong indicator for new particle formation bursts in a boreal forest.  
28 *Boreal Env. Res.* 21: 274–286, 2016.
- 29 Lelieveld, J., Berresheim, H., Borrmann, S., Crutzen, P., Dentener, F., Fischer, H., Feichter, J.,  
30 Flatau, P., Heland, J., Holzinger, R., Korrman, R., Lawrence, M., Levin, Z., Markowicz, K.,  
31 Mihalopoulos, N., Minikin, A., Ramanathan, V., de Reus, M., Roelofs, G., Scheeren, H., Sciare,  
32 J., Schlager, H., Schultz, M., Siegmund, P., Steil, B., Stephanou, E., Stier, P., Traub, M., Warneke,



- 1 C., Williams, J., and Ziereis, H.: Global air pollution crossroads over the Mediterranean,  
2 Science, 298, 794–799, doi: 10.1126/science.1075457, 2002.
- 3 Levelt, P. F., van den Oord, G. H. J., Dobber, M. R., Malkki, A., Visser, H., de Vries, J., Stammes,  
4 P., Lundell, J. O. V., and Saari, H.: The Ozone Monitoring Instrument, IEEE T. Geosci. Remote,  
5 44, 1093–1101, doi: 10.1109/TGRS.2006.872333, 2006.
- 6 Madronich, S.: The atmosphere and UV-B radiation at ground level. Environmental UV  
7 Photobiology, Plenum Press, 1–39, 1993.
- 8 Manninen, H.E., Nieminen, T., Asmi, E., Gagné, S., Häkkinen, S., Lehtipalo, K., Aalto, P., Kivekäs  
9 ,N., Vana, M., Mirme, A., Mirme, S., Hörrak, U., Plass-Dülmer, C., Stange, G., Kiss, G., Hoffer,  
10 A., Moerman, M., Henzing, B., Brinkenberg, M., Kouvarakis, G.N., Bougiatioti, K., O’Dowd, C.,  
11 Ceburnis, D., Arneth, A., Svenningsson, B., Swietlicki, E., Tarozzi, L., Decesari, S., Sonntag, A.,  
12 Birmili, W., Wiedensohler, A., Boulon, J., Sellegri, K., Laj, P., Baltensperger, U., Laaksonen, A.,  
13 Joutsensaari, J., Petäjä, T., Kerminen, V.-M., and Kulmala M.: EUCAARI ion spectrometer  
14 measurements at 12 European sites – analysis of new particle formation events, Atmos. Chem.  
15 Phys., 10, 7907-7927, 2010.
- 16 Mihalopoulos, N., Stephanou, E., Kanakidou, M., Pilitsidis, S., and Bousquet, P.: Tropospheric  
17 aerosol ionic composition in the eastern Mediterranean region, Tellus Series B - Chemical and  
18 Physical Meteorology, 49, 314– 326, 1997.
- 19 Mogensen, D., Gierens, R., Crowley, J. N., Keronen, P., Smolander, S., Sogachev, A., Nölscher,  
20 A. C., Zhou, L., Kulmala, M., Tang, M. J., Williams, J., and Boy, M.: Simulations of atmospheric  
21 OH, O<sub>3</sub> and NO<sub>3</sub> reactivities within and above the boreal forest, Atmos. Chem. Phys., 15, 3909-  
22 3932, <https://doi.org/10.5194/acp-15-3909-2015>, 2015.
- 23 Myriokefalitakis, S., Vignati, E., Tsigaridis, K., Papadimas, C., Sciare, J., Mihalopoulos, N.,  
24 Facchini, M. C., Rinaldi, M., Dentener, F. J., Ceburnis, D., Hatzianastasiou, N., O’Dowd, C.D.,  
25 van Weele, M., and Kanakidou, M.: Global modelling of the oceanic source of organic aerosols,  
26 Advances in Meteorology, doi:10.1155/2010/939171, 2010.
- 27 Myriokefalitakis S., Daskalakis, N., Fanourgakis, G. S., Voulgarakis, A., Krol, M. C., Aan de Brugh,  
28 J. M. J., and Kanakidou, M.: Pollution over the Mediterranean Basin: The Importance of Long-  
29 Range Transport on ozone and carbon monoxide, Science of The Total Environment, 563–564,  
30 40, 2016.



- 1 Nieminen, T., Asmi, A., Dal Maso, M., Aalto, P. P., Keronen, P., Petäjä, T., Kulmala, M., and  
2 Kerminen, V.-M.: Trends in atmospheric new-particle formation: 16 years of observations in a  
3 boreal-forest environment, *Boreal Env. Res.*, 19, 191-214, 2014
- 4 O'Dowd, C. D., Hämeri, K., Mäkelä, J. M., Pirjola, L., Kulmala, M., Jennings, S. G., Berresheim,  
5 H., Hansson, H.-C., de Leeuw, G., Kunz, G. J., Allen, A. G., Hewitt, C. N., Jackson, A., Viisanen,  
6 Y., and Hoffmann, T.: A dedicated study of New Particle Formation and Fate in the Coastal  
7 Environment (PARFORCE): Overview of objectives and achievements, *J. Geophys. Res.*, 107,  
8 8108, doi:10.1029/2001jd000555, 2002.
- 9 Paraskevopoulou, D., Liakakou, E., Gerasopoulos, E., and Mihalopoulos, N.: Sources of  
10 atmospheric aerosol from long-term measurements (5 years) of chemical composition in  
11 Athens, Greece. *Science of The Total Environment*, 527–528, 165–178.  
12 <http://doi.org/10.1016/J.SCITOTENV.2015.04.022>, 2015.
- 13 Petäjä, T., Kerminen, V.-M., Dal Maso, M., Junninen, H., Koponen, I.K., Hussein, T., Aalto, P.P.,  
14 Andronopoulos, S., Robin, D., Hämeri, K., Bartzis, J.G. and Kulmala, M.: Sub-micron  
15 atmospheric aerosols in the surroundings of Marseille and Athens: physical characterization  
16 and new particle formation, *Atmos. Chem. Phys.*, 7, pp. 2705-2720, doi:10.5194/acp-7-2705-  
17 2007, 2007.
- 18 Pikridas, M., Riipinen, I., Hildebrandt, L., Kostenidou, E., Manninen, H., Mihalopoulos, N.,  
19 Kalivitis, N., Burkhardt, J., Stohl, A., Kulmala, M. and Pandis, S. N.: NPF at a remote site in the  
20 eastern Mediterranean, *J. Geophys. Res.*, 117, D12205, doi:10.1029/2012JD017570, 2012.
- 21 Sciare, J., Bardouki, H., Moulin, C., and Mihalopoulos, N.: Aerosol sources and their  
22 contribution to the chemical composition of aerosols in the eastern Mediterranean Sea during  
23 summertime, *Atmos. Chem. Phys.*, 3, 291-302, <https://doi.org/10.5194/acp-3-291-2003>,  
24 2003.
- 25 Salimi, F., Rahman, M. M., Clifford, S., Ristovski, Z., and Morawska, L.: Nocturnal new particle  
26 formation events in urban environments. *Atmos. Chem. Phys.*, 17, 521–530.  
27 <http://doi.org/10.5194/acp-17-521-2017>, 2017.
- 28 Siakavaras, D., Samara, C., Petrakakis, M., and Biskos, G.: Nucleation events at a coastal city  
29 during the warm period: Kerbside versus urban background measurements. *Atmospheric*  
30 *Environment*, 140, 60–68. <http://doi.org/10.1016/j.atmosenv.2016.05.054>, 2016.



- 1 Spracklen, D. V., Carslaw, K. S., Kulmala, M., Kerminen, V.-M., Mann, G. W., and Sihto, S.-L.:  
2 The contribution of boundary layer nucleation events to total particle concentrations on  
3 regional and global scales, *Atmos. Chem. Phys.*, 6, 5631-5648, doi:10.5194/acp-6-5631-2006,  
4 2006.
- 5 Tammet, H., Komsaare, K., and Hörrak, U.: Intermediate ions in the atmosphere, *Atmospheric*  
6 *Research*, 135–136, 263–273, <http://doi.org/https://doi.org/10.1016/j.atmosres.2012.09.009>,  
7 2014.
- 8 Tröstl, J., Chuang, W. K., Gordon, H., Heinritzi, M., Yan, C., Molteni, U., Ahlm, L., Frege, C.,  
9 Bianchi, F., Wagner, R. and Simon, M., Lehtipalo, K., Williamson, C., Craven, J. S., Duplissy, J.,  
10 Adamov, A., Almeida, J., Bernhammer, A.-K., Breitenlechner, M., Brilke, S., Dias, A., Ehrhart,  
11 S., Flagan, R. C., Franchin, A., Fuchs, C., Guida, R., Gysel, M., Hansel, A., Hoyle, C. R., Jokinen,  
12 T., Junninen, H., Kangasluoma, J., Keskinen, H., Kim, J., Krapf, M., Kürten, A., Laaksonen, A.,  
13 Lawler, M., Leiminger, M., Mathot, S., Möhler, O., Nieminen, T., Onnela, A., Petäjä, T., Piel, F.  
14 M., Miettinen, P., Rissanen, M. P., Rondo, L., Sarnela, N., Schobesberger, S., Sengupta, K.,  
15 Sipilä, M., Smith, J. N., Steiner, G., Tomè, A., Virtanen, A., Wagner, A. C., Weingartner, E.,  
16 Wimmer, D., Winkler, P. M., Ye, P., Carslaw, K. S., Curtius, J., Dommen, J., Kirkby, J., Kulmala,  
17 M., Riipinen, I., Worsnop, D. R., Donahue, N. M., and Baltensperger, U.: The role of low-  
18 volatility organic compounds in initial particle growth in the atmosphere, *Nature*, 533, 527–  
19 531, 2016.
- 20 Tzitzikalaki, E., Kalivitis, N., Kouvarakis, G., Daskalakis, N., Kerminen, V.-M., Mihalopoulos, N.,  
21 Boy, M., and Kanakidou, M.: Simulations of New Particle Formation and Growth Processes at  
22 eastern Mediterranean, with the MALTE-Box Model, in: *Perspectives on Atmospheric*  
23 *Sciences*. T. Karacostas, A. Bais, & P. T. Nastos (Eds.), (pp. 933–939). Cham: Springer  
24 International Publishing, 2017.
- 25 Wang, Z., Wu, Z., Yue, D., Shang, D., Guo, S., Sun, J., Ding, A., Wang, L., Jiang, J., Guo, H., Gao,  
26 J., Cheung, H. C., Morawska, L., Keywood, M., and Hu, M.: New particle formation in China:  
27 Current knowledge and further directions, *Sci. Total Environ.*, 577, 258-266,  
28 <http://dx.doi.org/10.1016/j.scitotenv.2016.10.177>, 2017.
- 29 Wiedensohler, A., Birmili, W., Nowak, A., Sonntag, A., Weinhold, K., Merkel, M., Wehner, B.,  
30 Tuch, T., Pfeifer, S., Fiebig, M., Fjåraa, A. M., Asmi, E., Sellegri, K., Depuy, R., Venzac, H., Villani,  
31 P., Laj, P., Aalto, P., Ogren, J. A., Swietlicki, E., Williams, P., Roldin, P., Quincey, P., Hüglin, C.,  
32 Fierz-Schmidhauser, R., Gysel, M., Weingartner, E., Riccobono, F., Santos, S., Grüning, C.,



1 Faloon, K., Beddows, D., Harrison, R., Monahan, C., Jennings, S. G., O'Dowd, C. D., Marinoni,  
2 A., Horn, H.-G., Keck, L., Jiang, J., Scheckman, J., McMurry, P. H., Deng, Z., Zhao, C. S.,  
3 Moerman, M., Henzing, B., de Leeuw, G., Löschau, G., and Bastian, S.: Mobility particle size  
4 spectrometers: harmonization of technical standards and data structure to facilitate high  
5 quality long-term observations of atmospheric particle number size distributions, Atmos.  
6 Meas. Tech., 5, 657-685, doi:10.5194/amt-5-657-2012, 2012.

7



## 1 7) Tables

Day classification	Number of events	%
Total events	623	29.37
Class I	161	7.59
Class II	462	21.78
Undefined	555	26.17
Non-event	943	44.46
Total days	2121	100.00

2

3 Table 1) Total available measurement days and percentage of NPF events observed at  
 4 Finokalia during the period June 2008-June 2015

	$J_9$ ( $\text{cm}^{-3} \text{s}^{-1}$ )			$\text{GR}_{9-25}$ ( $\text{nm hr}^{-1}$ )			$\text{CS} \times 10^{-3}$ ( $\text{s}^{-1}$ )		
	Mean	Median	SD	Mean	Median	SD	Mean	Median	SD
Winter	0.7	0.6	0.4	3.3	2.7	2.2	3.7	3.1	2.6
Spring	0.9	0.8	0.6	3.5	2.7	2.5	5.5	5.1	2.7
Summer	0.7	0.6	0.4	6.8	6.4	3.5	9.1	8.9	3.7
Autumn	1.0	0.9	0.9	5.0	4.4	2.9	6.3	5.8	3.6

5

6 Table 2) Formation rates for 9nm particles ( $J_9$ ), growth rates in the size range 9-25 nm ( $\text{GR}_{9-25}$ )  
 7 for NPF events observed at Finokalia and condensational sink for sulphuric acid (CS) on  
 8 seasonal base during the period June 2008-June 2015 (mean, median and standard deviation).

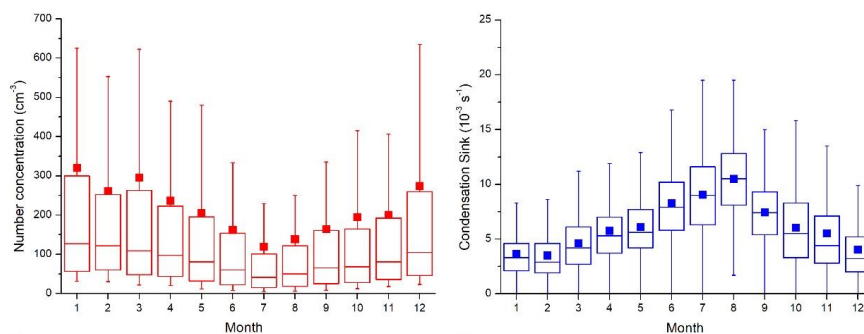
9

10

11



1 8) Figures

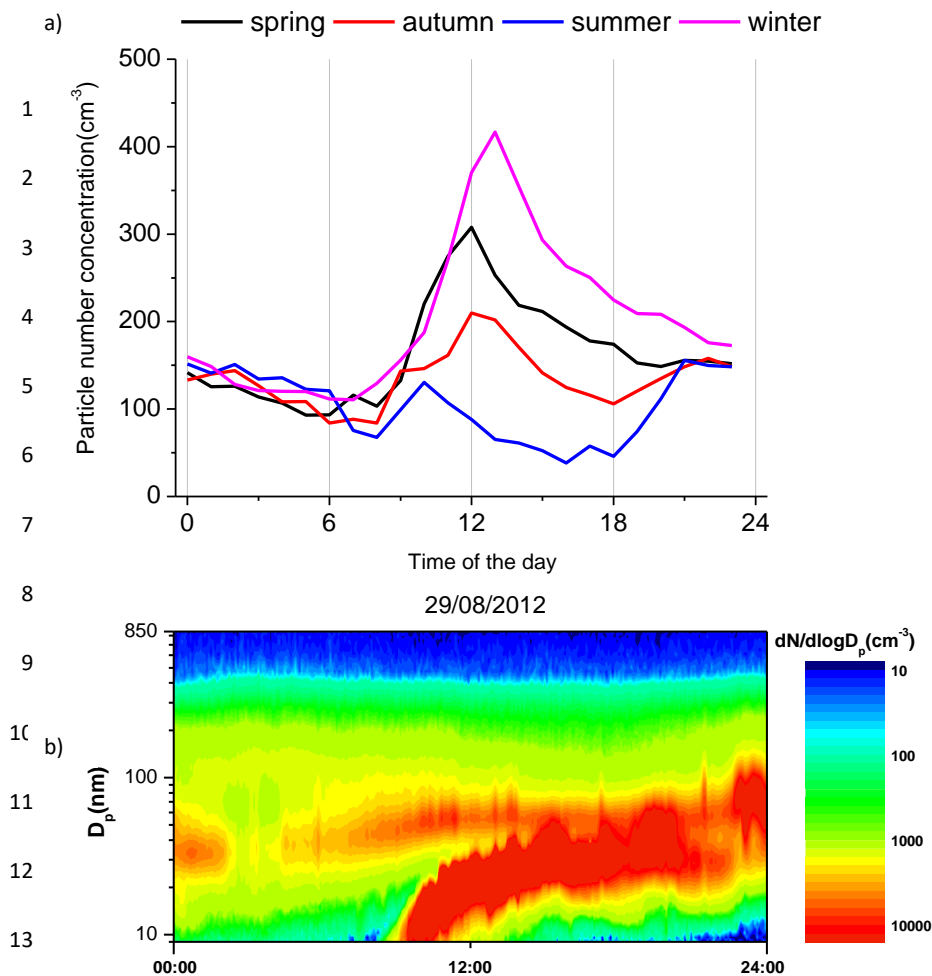


2 a)

b)

3 1) Monthly average variation of a) nucleation mode particle number concentration and b)  
4 sulfuric acid condensational sink (CS) at Finokalia station over the period June 2008-June 2015.  
5 Whiskers represent 10th and 90th percentiles, box edges are 75th and 25th percentiles, the  
6 line in the box is the median, the solid square is the mean.

7

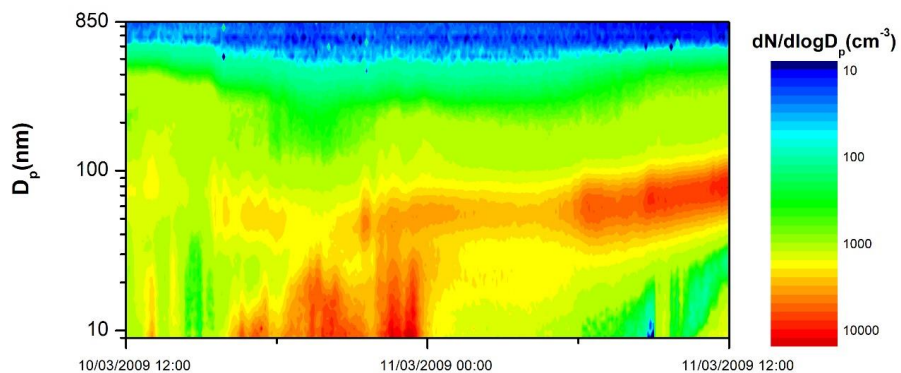


2) a) Average diurnal variation of nucleation mode particle number concentration (hourly values) at Finokalia over the period June 2008-June 2015 b) New particle formation event captured at Finokalia on 29/08/2012

21

22

23

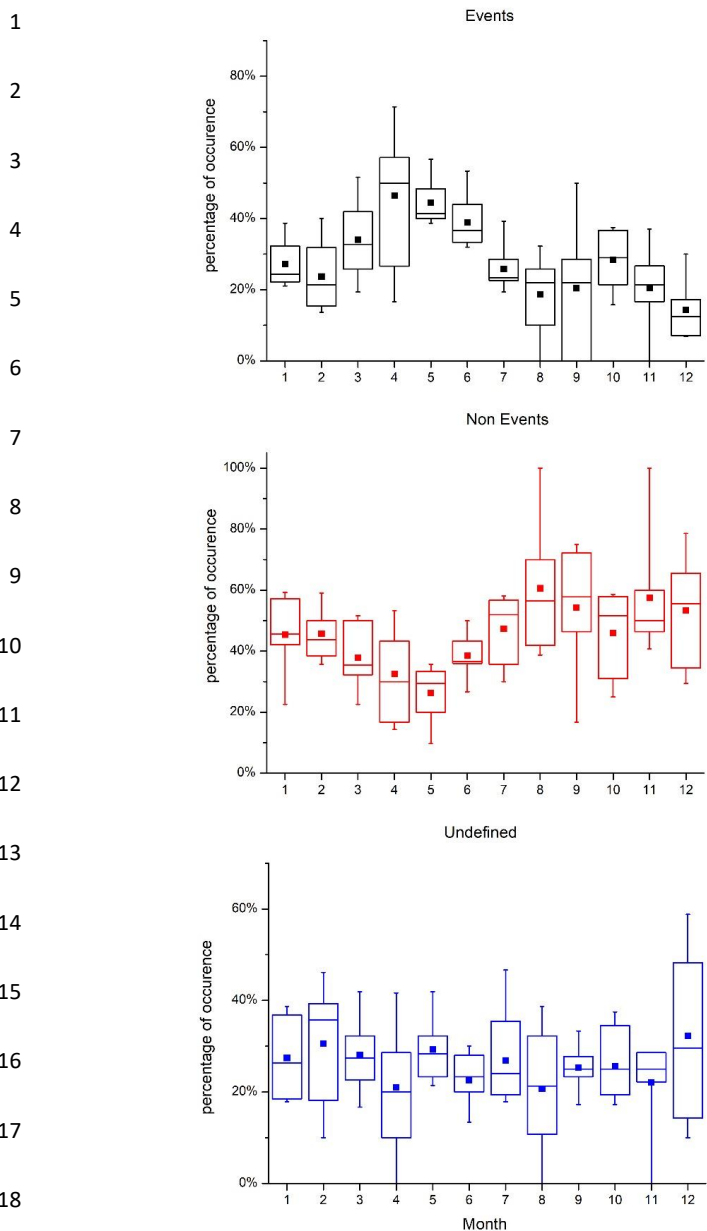


1

2 3) Example of appearance of nucleation mode particles during several hours as observed

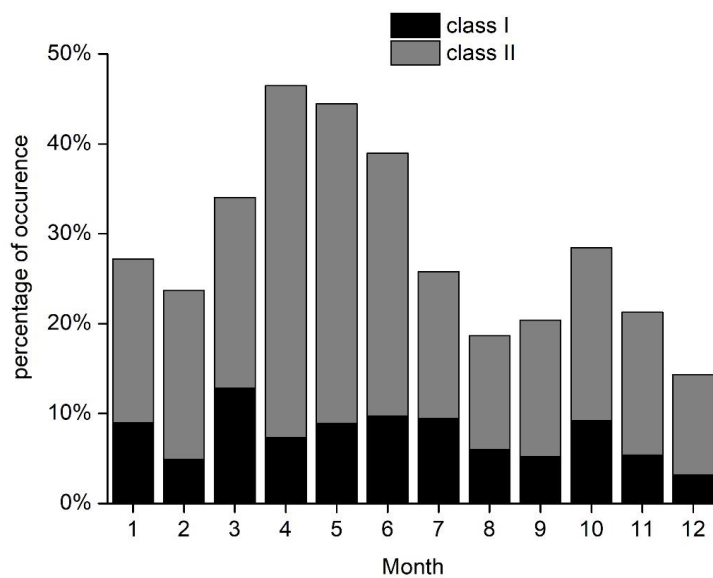
3 during the night of 10 to 11/09/2009.

4



19 4) Seasonal variation of NPF percentage of occurrence of event, non-event and undefined days  
 20 relatively to available measurement days at Finokalia for the period June 2008-June2015.  
 21 Whiskers represent 10th and 90th percentiles, box edges are 75th and 25th percentiles, the  
 22 line in the box is the median, square is mean.

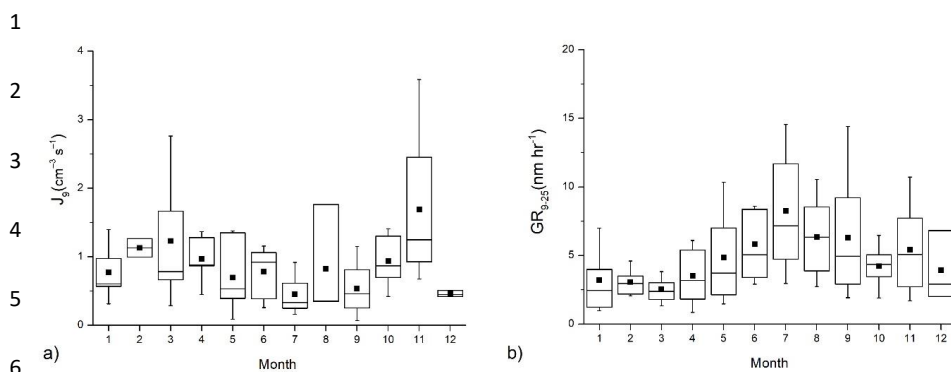
23



1

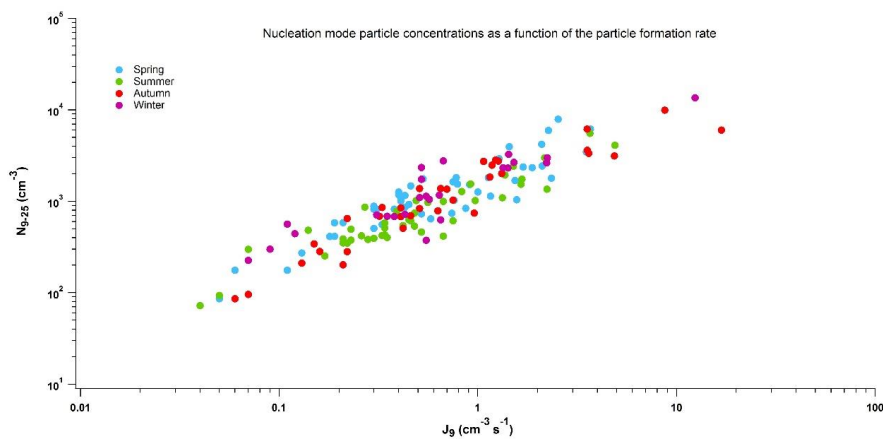
2 5) Seasonal variation of percentage of occurrence of NPF Class I & II events relatively to  
3 available measurement days at Finokalia in the eastern Mediterranean for the period June  
4 2008-June2015.

5



6) Seasonal variation of a) formation rate of 9nm particles ( $J_9$ ) and b) growth rate in the size range 9-25nm ( $GR_{9-25}$ ) as calculated during Class I NPF events at Finokalia for the period June 2008-June 2015. Whiskers represent 10th and 90th percentiles, box edges are 75th and 25th percentiles, the line in the box is the median and the solid square is the mean.

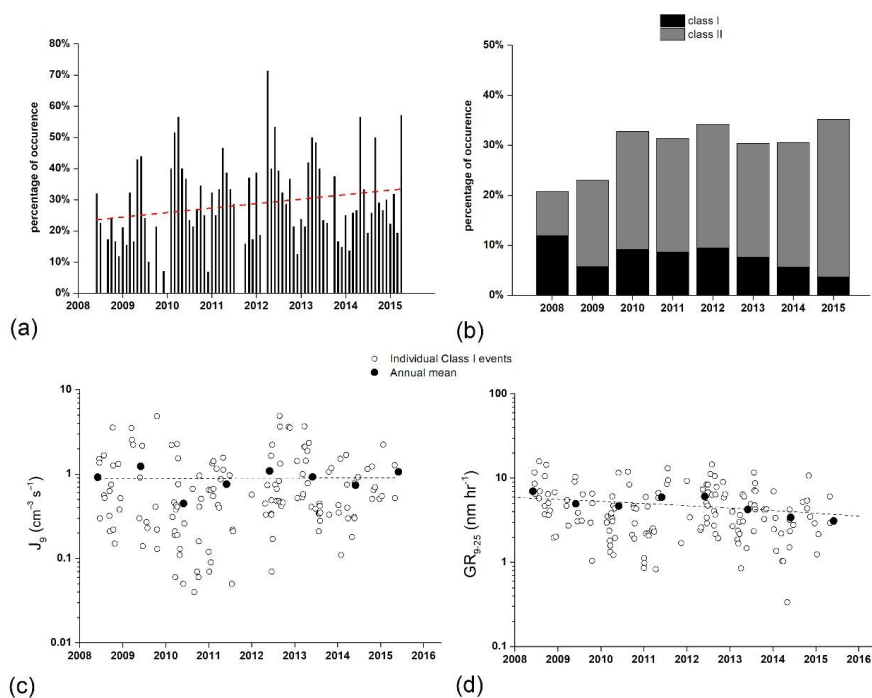
13



1

2 7) Scatter plot of formation rate of 9nm particles ( $J_9$ ) versus the number concentration of  
3 nucleation mode particles ( $N_{9-25}$ ) (hourly maximum value during the event) at Finokalia, for  
4 events that  $J_9$  could be calculated with a good level of confidence (Class I events).

5



1

2

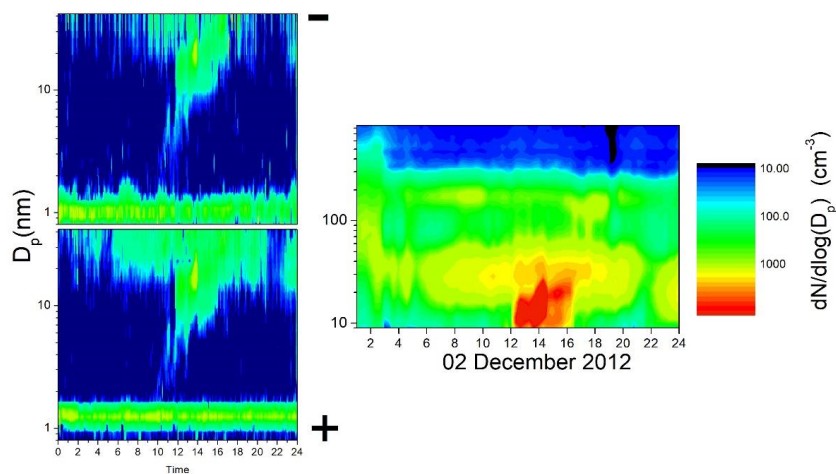
3 8) a) Time series of monthly NPF percentage of occurrence at Finokalia for the years 2008-  
 4 2015. b) Annual NPF percentage of occurrence at Finokalia for the period June 2008-June 2015  
 5 for Class I&II events. Interannual variation of c) formation rates of 9nm particles ( $J_9$ ) and d)  
 6 growth rate in the size range 9-25nm ( $GR_{9-25}$ ) during Class I NPF events at Finokalia for the  
 7 period June 2008-June 2015 (solid circles represent annual averages).

8



1

2



3

4

5

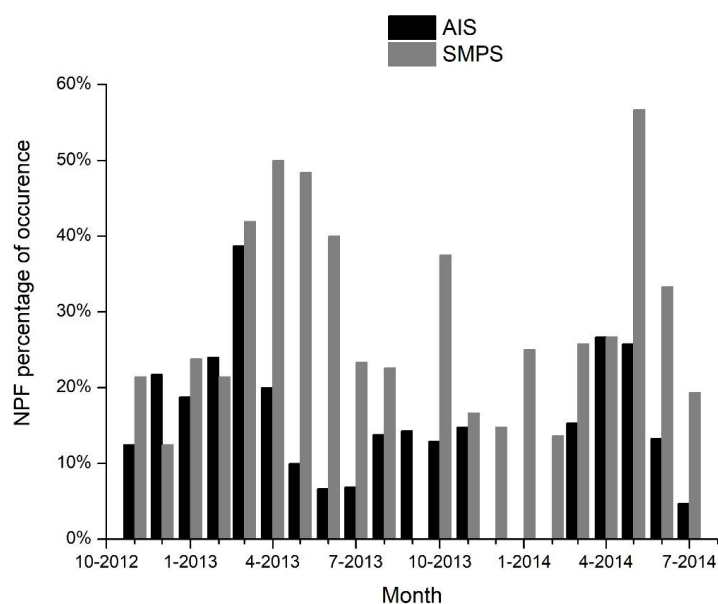
6 9) Nucleation event observed at Finokalia on 2 December 2012 as captured by AIS (left panels

7 for negative (up) and positive (bottom) polarity) and SMPS (right panel)

8



1



2

3 10) Monthly variability of NPF events' percentage of occurrence relatively to available  
4 measurement days at Finokalia as determined by analysis of AIS data during the FRONT  
5 experiment (Nov. 2012-July 2014). For a direct comparison, the monthly variability of NPF  
6 events as obtained from the SMPS measurements for the same period is included.

7



1

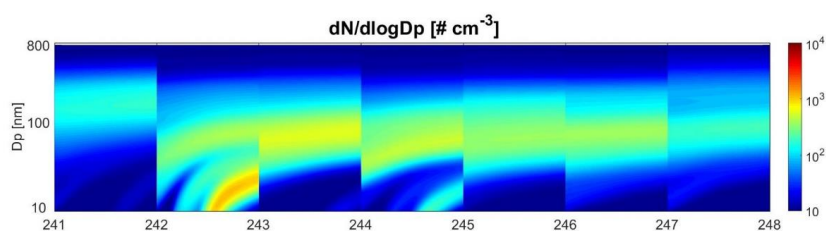
2

3

4

5

a)

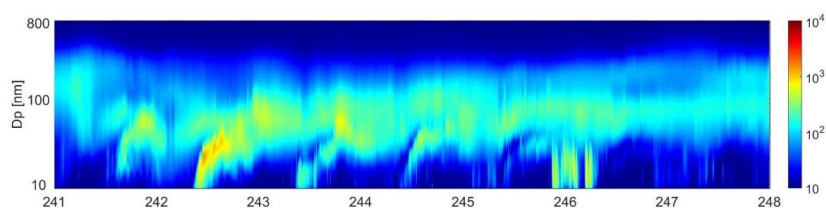


6

7

8

b)



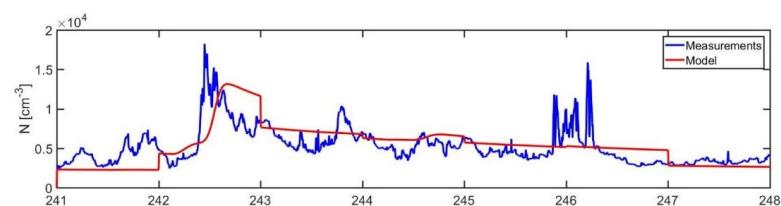
9

10

11

12

c)

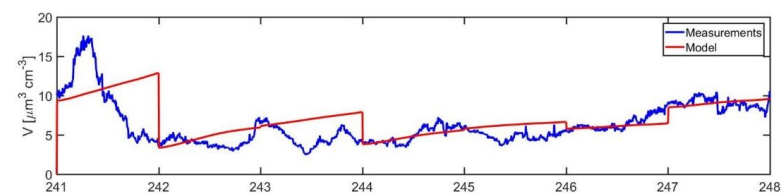


13

14

15

d)



16 11) Particle size distributions at Finokalia for the event week: a) simulations with the adjusted  
17 parameters for the sub-tropical environment The discontinuities observed every midnight in  
18 the model results are due to initialization of the model every midnight with measured number  
19 size distributions. b) observations of number size distributions (modified from Tzitzikalaki et  
20 al., 2017). Measured and modelled d) total number concentration and e) total volume  
21 concentration for the same period. The x-axis in all figures is Julian day of 2012.

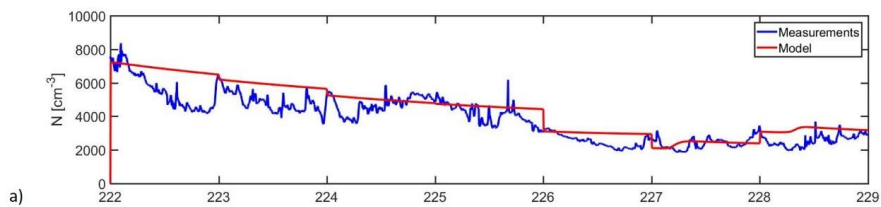


1

2

3

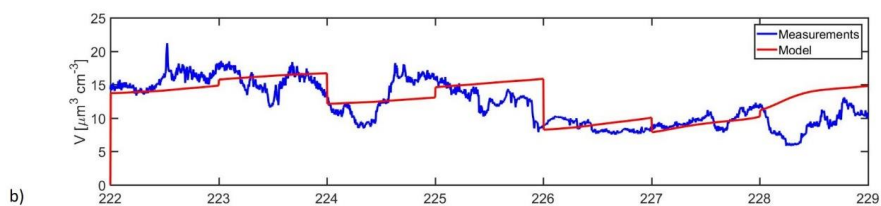
4



5

6

7



8

9 12) Measured and modelled a) total number concentration and b) total volume  
10 concentration for a non-event week at Finokalia. The x-axis in both figures is Julian day of  
11 2012.

12